Chemical solution deposition of single phase BiFeO₃ thin films on transparent substrates

Yaqiong Wang, Man Zhang, Yajun Yue, Hangfeng Zhang, Amit Mahajan, Steve Dunn*, Haixue Yan*

Y. Wang

Institute of Medical Engineering, Department of Biophysics, School of Basic Medical Sciences, Health Science Center, Xi'an Jiaotong University, Xi'an,710061, China

Y. Wang, M. Zhang, H. Zhang, A. Mahajan, H. Yan

School of Engineering and Materials Science, Queen Mary University of London, Mile End Road, London, E1 4NS, UK

E-mail: h.x.yan@qmul.ac.uk

Y. Yue

Department of Chemistry, Queen Mary University of London, Mile End Road London, E1 4NS, U.K.

Y. Wang, S. Dunn

Chemical and Energy Engineering, London South Bank University, 103 Borough Road, London SE1 0AA UK

E-mail: dunns4@lsbu.ac.uk

Abstract

The production of high quality BiFeO₃ thin films on cost-effective transparent electrodes for visible

light harvesting applications and devices remains a challenge. Here, we report the production of single-phase nanostructured $BiFeO_3$ thin films via chemical solution deposition (CSD) on transparent conductive fluorine doped tin oxide FTO glass substrates. We show that the $BiFeO_3$ is of high purity using a variety of analytical tools and that the as-obtained $BiFeO_3$ thin films have a single grain single domain structure exhibiting ferroelectric switching under poling. The $BiFeO_3$ samples show visible light absorption with a band gap of 2.7 eV under all processing conditions. By changing the annealing atmosphere it was possible to modify the photocurrent produced, which were (at 1.23 V_{NHE}) 0.07 mA/cm^2 (O_2-annealed), 0.02 mA/cm^2 (air-annealed) and 0.01 mA/cm^2 (Ar-annealed). This indicates a change in the mobile carriers available. Our results show that it is possible to produce single phase $BiFeO_3$ on a transparent conductive electrode system with controllable photoconductivity.

1. Introduction

Bismuth ferrite ($BiFeO_3$) is a ferroelectric material that has attracted much interest. Its multiferroic behaviour with a ferroelectric Curie point T_c = 1030 K and magnetic Neel temperature T_N = 670 K lead to a range of unusual and interesting properties.[1] $BiFeO_3$ is also known to be photoactive with a direct band gap around 2.7 eV and indirect bandgap around 2.2 eV. Both these band gaps are in the visible region of the solar spectrum. Between 2009 and 2012 it was found that $BiFeO_3$ thin films exhibit switchable ferroelectric diode behaviour with a visible light driven photovoltaic effect. This opens up opportunities for multi-functional devices that harvest or collect solar light and perform an energy conversion.[2] The synthesis of $BiFeO_3$ thin films is generally achieved using pulsed laser deposition,[3] radio-frequency sputtering,[4] molecular beam epitaxy[5] and metal organic chemical vapor deposition.[6] These methods have successfully produced $BiFeO_3$ films with low leakage current and low defect densities. They are not promising choices for large-scale $BiFeO_3$ thin film processing due to the expensive facilities needed and, in the case of chemical vapor deposition reported to date, complicated substrates preparation procedure. A low cost route for preparing high-quality $BiFeO_3$ thin films robust ferroelectric properties is a key and vital next step for many practical applications.

Chemical solution deposition (CSD) is a common method for fabricating functional thin films that can have controlled thicknesses in the nm range or tailored surface morphology.[7] It has the advantages of easy fabrication and is scalable for large area film synthesis. It is well known that $BiFeO_3$ can easily form parasitic phases and defects with a variety of reasons being suggested.[8] $BiFeO_3$ has been reported as being metastable, off-stoichiometric and easy to lose Bi during annealing. This leads to secondary phases or a highly conductive film with high leakage.[8a, 9] The control of $BiFeO_3$ phase becomes more challenging when using CSD since the precipitation of impurity phases can happen during the heating cycle of film synthesis. Impurity phases compromise the functional performance of $BiFeO_3$. For example, $BiFeO_3$ films with Fe_2O_3 show a ferromagnetic behaviour rather than the low bulk-like magnetic moment exhibited by single-phase $BiFeO_3$ films. Growth of conductive Bi_2O_3 creates electric short circuit through the $BiFeO_3$ film.[8b] Dedicated control of the film gelation process to obtain a homogeneous gel film before annealing has been suggested to be critical for CSD-synthesised epitaxial $BiFeO_3$ film.[10] One general recipe used is to use a slightly higher Bi:Fe ratio than 1:1 producing a Bi-excess in the films. This compensates for Bi losses during annealing and suppresses the formation of Bi and O vacancies.[11] O_2 has been used as the annealing atmosphere to compensate for oxygen vacancy formation.[12] However, these additional processing steps bring problems such as the formation of bismuth-rich phases or increase the cost and complexity for the fabrication of the thin films.

In applications such as solar active devices and photochemical cells the system often requires transparent electrodes to enable light to activate the film via the back interface.[13] In these instances the $BiFeO_3$ thin film needs to be produced on industry standard transparent substrates such as fluorine doped tin oxide (FTO) or indium doped tin oxide (ITO) coated glass. Deposition of a $BiFeO_3$ thin film on readily available, transparent and conductive FTO glass is a preferable choice for wide range of applications.

Here we demonstrate that we produce high quality $BiFeO_3$ film which is a single phase. The photoelectrochemical properties of the $BiFeO_3$ thin films annealed under oxygen, air and argon were studied and are shown to be compatible with previous studies for $BiFeO_3$ films. The ferroelectric

property of the BiFeO$_3$ thin film was characterised using piezoresponse force microscopy (PFM) and switchable polarisation was demonstrated. This is indicative of the as-prepared BiFeO$_3$ films having good ferroelectric properties. The results provide a CSD approach to prepare polycrystalline BiFeO$_3$ thin films. This paves the way to use the material in photovoltaic, photochemical and ferroelectric devices.

2. Results and discussion

We have used acetic anhydride as the dehydration agent and carefully controlled the substrate temperature during gelation. Through this process we have successfully produced a BiFeO$_3$ thin film on FTO coated glass that has properties consistent with a previous report on single crystal substrates.[10] A photo of the BiFeO$_3$ film (**Figure S1**) demonstrates its good transparency. A review of the X-ray diffraction patterns (**Figure 1**) shows that a polycrystalline single-phase BiFeO$_3$ film has been produced after annealing in oxygen, air and argon. It is not necessary to have an oxygen-rich atmosphere to produce high purity BiFeO$_3$ thin films.

Looking at the X-ray diffraction (XRD) patterns, Figure 1, of the as-annealed BiFeO$_3$ thin films in more detail we find all the films show well-crystallized rhombohedral structures. This match and the absence of secondary-phase peaks demonstrate the high purity of the samples. Close investigation of the (012) peak for the three annealing regimes shows some differences. In the case of the Ar-annealed sample there is a higher intensity of the (012) peak compared to the (104)/(110) peaks. For the O$_2$- and air- annealed BiFeO$_3$, the (012) has a lower relative intensity to (104)/(110), which suggests that different annealing atmosphere can lead to different orientation for grain growth. Similar effect of different annealing atmosphere on orientation of grain growth was also reported in the work by Thundat et. al.[14] The refinement of crystal structures was carried out by means of the GSAS software suite,[15] to evaluate the effect of the annealing atmosphere on crystal structure of BiFeO$_3$. A rhombohedral model (α = 5.58197(3) Å and c =13.87773(9) Å in the space group $R3c$) was applied in structure refinements.[16] The refinement results are shown in **Figure S2**, to allow the comparison of ferroelectric distortion for BiFeO$_3$ annealed at different atmosphere, all the lattice parameters were

converted to pseudocubic equivalent cell with $a_{PC} = a_R/\sqrt{2}$ and $c_{PC} = c_R/2\sqrt{3}$ and $V_{PC} = V_R/6$. The crystal structure distortion (c_{PC}/a_{PC}) of O_2-, air- and Ar- annealed $BiFeO_3$ are 1.0148, 1.0148 and 1.0151 (details shown in **Table S1**), respectively. The distortion values are very close, indicating that annealing in the three different atmospheres did not change the long-range crystallographic structure of the $BiFeO_3$ thin films.
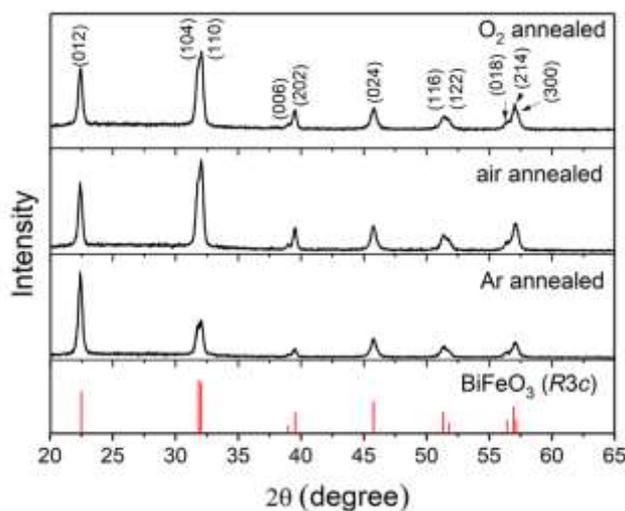
Figure 1. XRD patterns of $BiFeO_3$ thin films annealed in O_2, air and Ar.

Figure 2 shows scanning electron micro-scope (SEM) images of the $BiFeO_3$ thin films annealed. The SEM images on a microscopic scale can be found in **Figure S3**. The $BiFeO_3$ films exhibit a polycrystalline and compact morphology with the grain size ranging from around 50 nm to 300 nm for samples produced under all annealing atmospheres. This observation differs from previous reports that indicate an O_2 atmosphere is essential for the preparation of $BiFeO_3$ thin films with high quality crystallization. It is rare to see a compact morphology due to the difficulty in $BiFeO_3$ synthesis although under our process we have achieved a high-quality film. Achieving a dense morphology is important for applications of $BiFeO_3$ thin films especially when nanostructured or produced with nm level cross section. It is necessary to produce a film without holes or voids to minimize electrical short circuits in the device.[17]
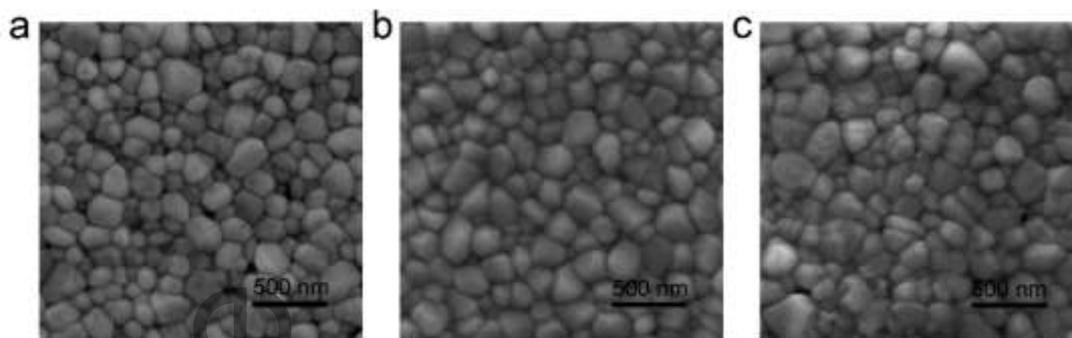
Figure 2. SEM images of BiFeO$_3$ films. (a) O$_2$-annealed (b) air-annealed (c) Ar-annealed.

To investigate effect of the annealing atmosphere on the oxidation state of Fe and O, X-ray photoelectron spectroscopy (XPS) was performed on the as-prepared BiFeO$_3$ thin films. The fitted Fe 2p and O1s spectra for the three samples are shown in **Figure 3**. The fitting data of Fe 2p and O 1s are summarized in **Table S2 and S3**. The characteristic 2p$_{3/2}$ and 2p$_{1/2}$ peaks of Fe were separated by 13.6 eV.[18] The Fe 2p$_{1/2}$ (~ 730 eV) and Fe 2p$_{3/2}$ (~ 718 eV) satellites peaks occur at the high-bingding-energy side of each main peak. Two peaks located at ~ 712 eV (characteristic peak of Fe^{3+}) and ~ 710 eV (characteristic peak of Fe^{2+}) are obtained after fitting of Fe 2p$_{3/2}$ peaks of three samples, indicating that Fe^{2+} exists in all three samples. A review of Table S2 shows that valence of Fe relates to the film annealing atmosphere, and more Fe^{2+} formed under oxygen deficient condition, which is consistent with previous studies.[19] The production of more Fe^{2+} can be related to a higher defect density in the sample. The O1s peak can be resolved into two subpeaks located around 529 eV and 531, corresponding to the lattice oxygen and oxygen associated with oxygen vacancies.[20] The Ar-annealed sample shows an additional peak at ~ 532 eV, which can be attributed to oxygen bonded to carbon.[21] Comparing the peak area in Table S2 it can be seen that annealing in oxygen-deficient atmosphere resulted in more oxygen vacancies. Analysis of the Fe 2p and O 1s XPS spectra indicates that annealing in oxygen-deficient atmosphere results in more Fe^{2+} with consequent formation of oxygen vacancies.
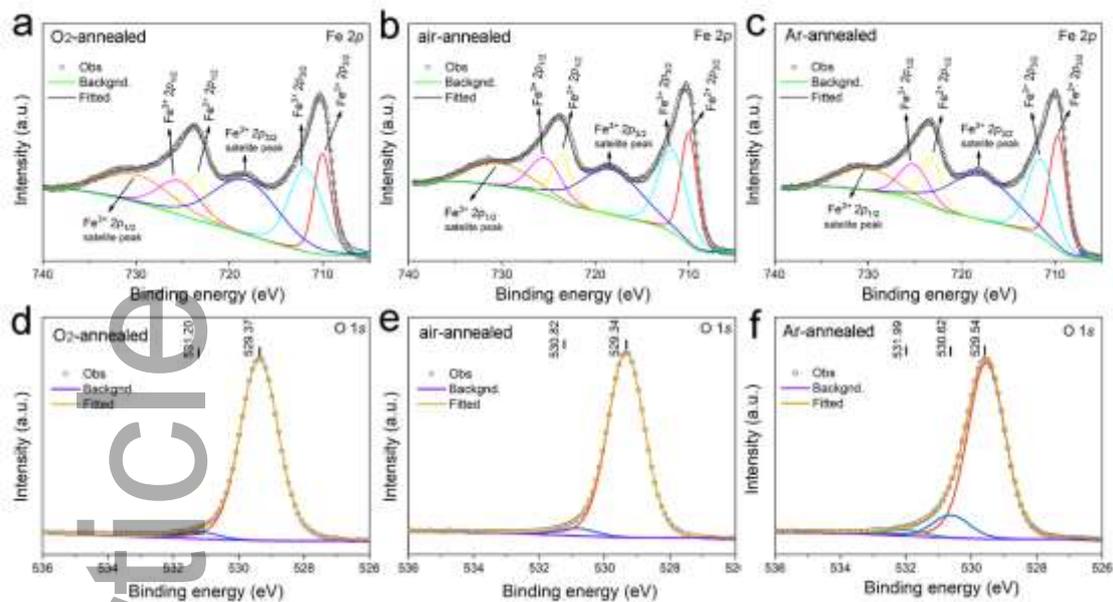
Figure 3. Fe 2*p* and O 1*s* XPS spectra of the BiFeO$_3$ films annealed in O$_2$ (a, d), air (b, e) and Ar (c, f).

The domain structure and switching properties of the BiFeO$_3$ thin films were characterised by piezoelectric force microscopy (PFM), shown in **Figure 4** and **Figure S3**. Phase image shows bright and dark contrast corresponds to the domain orientation towards and opposite to the applied field direction. It can be seen from the topography and phase (domain) images that the BiFeO$_3$ thin films have a single domain structure within one grain. This suggests that the grain size is too small to produce domain walls within a grain.[22] This unique single-domain-single-grain polycrystalline structure can be used for a mechanistic study of polycrystalline BiFeO$_3$ film in multi-functional applications without a domain wall contribution.[23]
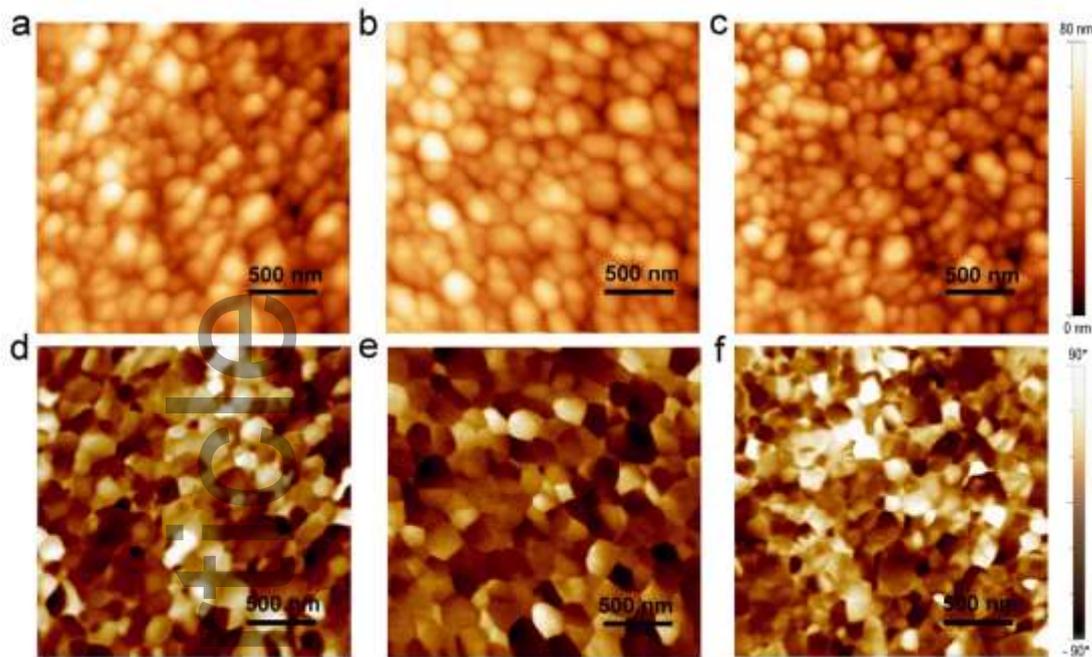
Figure 4. Topography (a, b, c) and phase images (d, e, f) of BiFeO$_3$ thin films annealed in O$_2$ (a, d), air (b, e) and Ar (c, f).

Figure 5a shows the UV-vis spectra of the three thin films with Figure 5b showing the derived Tauc-plots. From the absorption spectra it can be seen that the BiFeO$_3$ thin films annealed in different atmospheres have a very close light absorption onset and show good visible light absorption. Tauc plots in Figure 5b show that the three samples have a consistent band gap value of around 2.7 eV. This characterisation indicates that the annealing atmosphere does not make significant differences to the band gap of the thin films. It should be noted that band gap of BiFeO$_3$ has many reported values ranging from 2.1 eV to 2.8 eV, owning to its complex defect nature. Typically the loss of Bi and O during annealing or the valence change of Fe lead to a change in band gap.[1a, 24] The atmosphere used during annealing has been shown to affect the defect structure of BiFeO$_3$ by influencing Bi and O loss. The results here suggest that controlling those conditions with a short annealing duration of 1h and a low annealing temperature of 650 °C it is possible to remove the influence of atmosphere on band gap.

The photochemical properties of the BiFeO$_3$ thin films were characterised in a photoelectrochemical (PEC) cell. Figure 5c shows the photocurrent-voltage (J-V) curves of BiFeO$_3$ thin films illuminated

under chopped AM1.5G illumination. The photocurrents at 1.23 V_{NHE} were 0.07 mA/cm^2 (O$_2$-annealed), 0.02 mA/cm^2 (air-annealed) and 0.01 mA/cm^2 (Ar-annealed). These are comparable to previously reported photocurrents of BiFeO$_3$ films prepared by PLD (0.06 mA/cm^2 at 1.1 V_{NHE} under 1 sun)[25], sputtering (0.01 mA/cm^2 at 1 V_{NHE} under 1 sun)[26] and hydrothermal (5.2 µA/cm^2 at 1.0 V vs. SCE, 500 W Hg lamp) method.[27] The good performance can be attributed to the compact morphology and well crystallized structure. The J-V results demonstrate that BiFeO$_3$ thin films prepared by CSD method are promising candidates for photochemical applications.

The photocurrents show a decreasing trend with the annealing atmosphere changing from O$_2$ to air and Ar. When the applied voltage reached 1.4 V_{NHE}, the dark currents of all samples increased. This was most notable in the Ar-annealed sample. This is indicative of highly mobile carrier flow through the film. We relate this to the increased Fe^{2+} content in the films annealed under oxygen-deficient condition as indicated in the XPS results. Electrons in the BiFeO$_3$ film can hop between Fe^{2+} and Fe^{3+} sites and result in a conducting behavior.[28] This acts to compromise the photochemical performance and ferroelectric properties of the film. The BiFeO$_3$ films here were prepared by repeating the precursor solution deposition procedure five times and the obtained thickness was around 150 nm, observed under SEM. The choice of 5 layers was optimized from our earlier experimental work. A thinner BiFeO$_3$ film prepared by depositing less than 5 layers showed large dark/leakage currents due to bad film coverage on FTO surface while a thicker film showed limited photocurrents due to the weak hole transport ability under back-side illumination. It was demonstrated by Pala et. al. that the back-side illuminated photocurrents decay exponentially with respect to the film thickness.[29] This is attributed to the short hole diffusion length of the material (typically a few nanometers).[30]
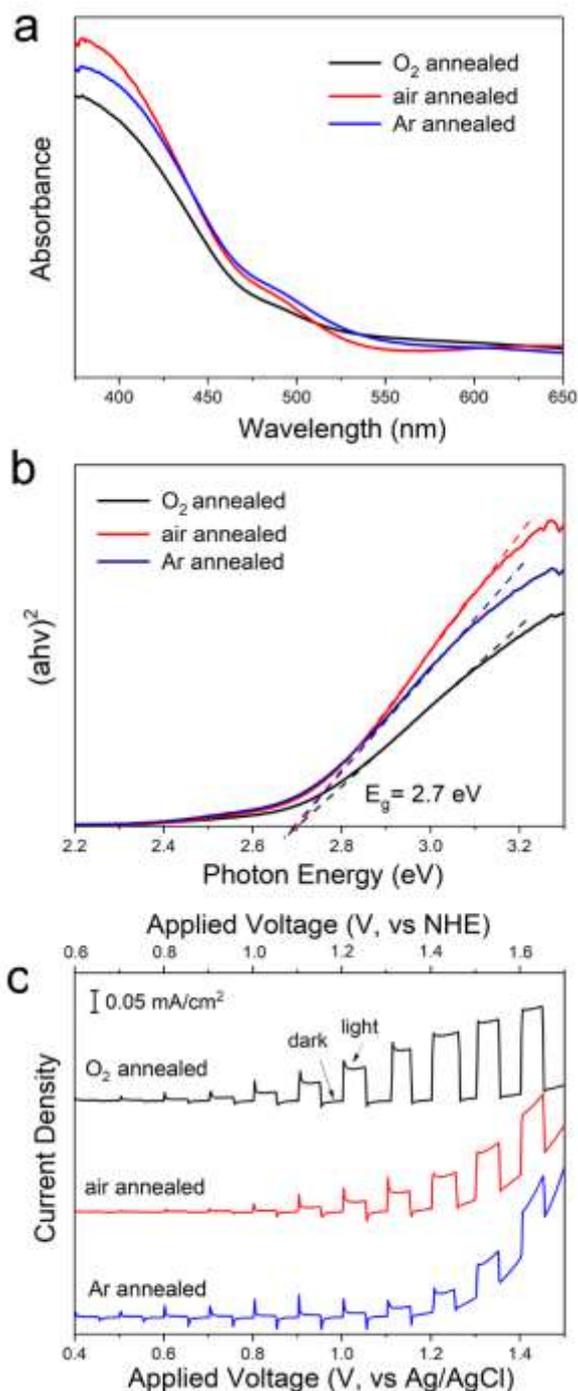
Figure 5. (a) UV-vis absorption spectra of the BiFeO₃ films annealed in O₂, air and Ar. (b) Tauc plots derived from the UV vis absorption spectra. (c) J-V curve for BiFeO₃ films annealed in O₂, air and Ar under full AM1.5G chopped illumination. Noted that the samples were prepared following the identical procedures and conditions, the only difference was the annealing atmosphere used.

It is worth noting that current spikes are observed in all the three samples under low applied bias. These include positive spikes when switching from dark to light and negative spikes from light to

dark. These spikes have been attributed to the surface recombination of photoexcited carriers.[31] The positive spikes were resulted from the accumulation of holes at the electrode/electrolyte interface, which injected to the electrolyte once light on. While the later decreased but steady photocurrents were generated by holes diffused to the interface, which have a kinetic limitation. The negative spikes, likewise, were generated by the back reaction of electrons from the conduction band with the accumulated holes. At higher potentials, the spikes disappeared since the carries obtained enough driving force and the holes reached the surface can inject into the electrolyte more freely. This behavior is in turn related to the surface traps or defects.[32] In general the current spike scale of O_2-annealed sample is smaller than the air-annealed sample. The largest current spike is for the Ar-annealed sample. This adds more evidence to the XPS data to indicate that higher O_2 annealing leads to a reduced number of traps and defect densities. Thus, while the atmosphere of anneal does not change the phase pure nature of the $BiFeO_3$ a higher O_2 annealing atmosphere is preferable for $BiFeO_3$ photoelectrode processing.

3. Conclusion

$BiFeO_3$ thin films on FTO glass substrates were successfully fabricated via a CSD method. We show that pure phase $BiFeO_3$ thin film can be produced in either oxygen-rich or deficient annealing atmospheres. The $BiFeO_3$ thin films show a direct band gap value of 2.7 eV irrespective of annealing atmosphere. The $BiFeO_3$ thin films show single domain polycrystalline structure due to the small grain size. PFM characterization of the $BiFeO_3$ thin films demonstrated they have a ferroelectric nature. The $BiFeO_3$ thin films exhibit good photochemical performance. There was a noticeable relationship between the annealing atmosphere and measured photocurrent due to the variations in defect density associated with annealing. Our results demonstrate that it is possible to fabricate high quality $BiFeO_3$ thin films via a simple CSD method. We demonstrate a promising technique for large-area $BiFeO_3$ thin films in memory device, photochemistry and photovoltaic areas.

Acknowledgements

References

[1] a) G. Catalan, J. F. Scott, *Adv. Mater.* **2009**, *21* (24), 2463; b) J. Wang, J. B. Neaton, H. Zheng, V. Nagarajan, S. B. Ogale, B. Liu, D. Viehland, V. Vaithyanathan, D. G. Schlom, U. V. Waghmare, N. A. Spaldin, K. M. Rabe, M. Wuttig, R. Ramesh, *Science* **2003**, *299* (5613), 1719.

[2] a) T. Choi, S. Lee, Y. J. Choi, V. Kiryukhin, S.-W. Cheong, *Science* **2009**, *324* (5923), 63; b) S. Y. Yang, L. W. Martin, S. J. Byrnes, T. E. Conry, S. R. Basu, D. Paran, L. Reichertz, J. Ihlefeld, C. Adamo, A. Melville, Y.-H. Chu, C.-H. Yang, J. L. Musfeldt, D. G. Schlom, J. W. Ager, R. Ramesh, *Appl. Phys. Lett.* **2009**, *95* (6), 062909; c) R. Moubah, O. Rousseau, D. Colson, A. Artemenko, M. Maglione, M. Viret, *Adv. Funct. Mater.* **2012**, *22* (22), 4814.

[3] A. Q. Jiang, C. Wang, K. J. Jin, X. B. Liu, J. F. Scott, C. S. Hwang, T. A. Tang, H. B. Lu, G. Z. Yang, *Adv. Mater.* **2011**, *23* (10), 1277.

[4] R. Y. Zheng, X. S. Gao, Z. H. Zhou, J. Wang, *J. Appl. Phys.* **2007**, *101* (5), 054104.

[5] J. F. Ihlefeld, N. J. Podraza, Z. K. Liu, R. C. Rai, X. Xu, T. Heeg, Y. B. Chen, J. Li, R. W. Collins, J. L. Musfeldt, X. Q. Pan, J. Schubert, R. Ramesh, D. G. Schlom, *Appl. Phys. Lett.* **2008**, *92* (14), 142908.

[6] R. Ueno, S. Okaura, H. Funakubo, K. Saito, *Jpn. J. Appl. Phys.* **2005**, *44* (No. 39), L1231.

[7] C. J. Brinker, G. W. Scherer, *Sol-gel science: the physics and chemistry of sol-gel processing*, Academic press, Boston **1990**.

[8] a) M. Valant, A.-K. Axelsson, N. Alford, *Chem. Mater.* **2007**, *19* (22), 5431; b) H. Béa, M. Bibes, A. Barthélémy, K. Bouzehouane, E. Jacquet, A. Khodan, J.-P. Contour, S. Fusil, F. Wyczisk, A. Forget, D. Lebeugle, D. Colson, M. Viret, *Appl. Phys. Lett.* **2005**, *87* (7), 072508.

[9] S. Iakovlev, C.-H. Solterbeck, M. Kuhnke, M. Es-Souni, *J. Appl. Phys.* **2005**, *97* (9), 094901.

[10] Q. Zhang, N. Valanoor, O. Standard, *J. Mater. Chem. C* **2015**, *3* (3), 582.

[11] a) L. R. Dedon, S. Saremi, Z. Chen, A. R. Damodaran, B. A. Apgar, R. Gao, L. W. Martin, *Chem. Mater.* **2016**, *28* (16), 5952; b) J. Li, N. Sha, Z. Zhao, *Appl. Surf. Sci.* **2018**, *454*, 233.

[12] Q. Zhang, N. Valanoor, O. Standard, *J. Appl. Phys.* **2014**, *116* (6), 066810.

[13] T. R. Harris-Lee, Y. Zhang, C. R. Bowen, P. J. Fletcher, Y. Zhao, Z. Guo, J. W. F. Innocent, S. A. L. Johnson, F. Marken, *Electrocatalysis* **2021**, *12* (1), 65.

[14] K. Prashanthi, M. Gupta, Y. Y. Tsui, T. Thundat, *Appl. Phys. A* **2013**, *110* (4), 903.

[15] A. C. V. D. Larson, R. B., GSAS Generalised Structure Analysis System; Los Alamos National Laboratory: Report. **1987**.

[16] R. C. Lennox, M. C. Price, W. Jamieson, M. Jura, A. Daoud-Aladine, C. A. Murray, C. Tang, D. C. Arnold, *J. Mater. Chem. C* **2014**, *2* (17), 3345.

[17] I. C. Yao, D.-Y. Lee, T.-Y. Tseng, P. Lin, *Nanotechnology* **2012**, *23* (14), 145201.

[18] J. F. Moulder, W. F. Stickle, W. M. Sobol, K. D. Bomben, *Perkin-Elmer* **1992**, *40*, 221.

[19] I. S. Golovina, M. Falmbigl, A. V. Plokhikh, T. C. Parker, C. Johnson, J. E. Spanier, *J. Mater. Chem. C* **2018**, *6* (20), 5462.

[20] P. S. V. Mocherla, C. Karthik, R. Ubic, M. S. Ramachandra Rao, C. Sudakar, *Appl. Phys. Lett.* **2013**, *103* (2), 022910.

[21] Y. Wang, Y. Pu, X. Li, H. Zheng, Z. Gao, *Mater. Chem. Phys.* **2016**, *183*, 247.

[22] a) Z. Zhao, V. Buscaglia, M. Viviani, M. T. Buscaglia, L. Mitoseriu, A. Testino, M. Nygren, M. Johnsson, P. Nanni, *Phys. Rev. B* **2004**, *70* (2), 024107; b) Q. Jiang, H. Ning, Q. Zhang, M. Cain, M. J. Reece, H. Yan, *J. Mater. Chem. C* **2013**, *1* (36), 5628.

[23] Y. Wang, M. Zhang, J. Liu, H. Zhang, F. Li, C.-W. Tseng, B. Yang, G. Smith, J. Zhai, Z. Zhang, S. Dunn, H. Yan, *Adv. Energy Mater.* **2020**, *10* (38), 2001802.

[24] a) S. J. Clark, J. Robertson, *Appl. Phys. Lett.* **2007**, *90* (13), 132903; b) *Appl. Phys. Lett.* **2009**, *94* (2), 022902.

[25] L. T. Quynh, C. N. Van, Y. Bitla, J.-W. Chen, T. H. Do, W.-Y. Tzeng, S.-C. Liao, K.-A. Tsai, Y.-C. Chen, C.-L. Wu, C.-H. Lai, C.-W. Luo, Y.-J. Hsu, Y.-H. Chu, *Adv. Energy Mater.* **2016**, *6* (18), 1600686.

[26] W. Ji, K. Yao, Y.-F. Lim, Y. C. Liang, A. Suwardi, *Appl. Phys. Lett.* **2013**, *103* (6), 062901.

[27] U. A. Joshi, J. S. Jang, P. H. Borse, J. S. Lee, *Appl. Phys. Lett.* **2008**, *92* (24), 242106.

[28] S. R. Basu, L. W. Martin, Y. H. Chu, M. Gajek, R. Ramesh, R. C. Rai, X. Xu, J. L. Musfeldt, *Appl.*

Phys. Lett. **2008**, *92* (9), 091905.

[29] R. A. Pala, A. J. Leenheer, M. Lichterman, H. A. Atwater, N. S. Lewis, *Energy Environ. Sci.* **2014**, *7* (10), 3424.

[30] L. Wang, H. Ma, L. Chang, C. Ma, G. Yuan, J. Wang, T. Wu, *Small* **2017**, *13* (1), 1602355.

[31] P. Iwanski, J. S. Curran, W. Gissler, R. Memming, *J. Electrochem. Soc.* **1981**, *128* (10), 2128.

[32] H. Dotan, K. Sivula, M. Gratzel, A. Rothschild, S. C. Warren, *Energy Environ. Sci.* **2011**, *4* (3), 958.

Photocurrents from nanostructured BiFeO$_3$ films produced using low-cost chemical solution deposition indicate a photoactive material. By developing a chemical solution deposition process for BiFeO$_3$ we enable the production of high quality multi-ferroic thin films for a range of applications where a narrow band gap photoactive material is needed. Our process removes the need for an anneal in a controlled atmosphere.